ISBN: 978-3-95450-247-9 ISSN: 2673-5490 doi: 10.18429/JACoW-IPAC2024-WEPC65

MONTE CARLO MODELING OF SPIN-POLARIZED PHOTOEMISSION FROM GaAs WITH LOW-TEMPERATURE AND STRAINED-LATTICE EFFECTS

J. Callahan*, O. Chubenko†, Northern Illinois University, DeKalb, IL, USA
L. Cultera, Brookhaven National Laboratory, Upton, NY, USA
S. Karkare, Arizona State University, Tempe, AZ, USA
A. Rodriguez Alicea, University of Michigan, Ann Arbor, MI, USA
J. O. Mendez-Nieves, University of Puerto Rico - Rio Piedras, San Juan, PR, USA

Abstract

The degree of spin-polarization of electrons photoemitted from unstrained GaAs is usually considerably less than the theoretical maximum of 50 %. However, it has been experimentally observed that the degree of electron spin polarization can be increased and even exceed the theoretical maximum when the sample is cooled to low temperatures. Additionally, in strained lattice samples, the theoretical maximum of spin polarization increases to 100 %. The previously developed Monte Carlo approach to spin-polarized photoemission from unstrained, room temperature negative electron affinity (NEA) GaAs provides excellent agreement with experimental data in a wide range of doping densities and photoexcitation energies. This study aims to extend the model's capabilities by incorporating both low-temperature and strained-lattice effects into the band structure and exploring their impact on spin and momentum relaxation mechanisms. We report on the Monte Carlo modeling of electron drift velocity, quantum efficiency (QE), and electron spin-polarization (ESP) of bulk GaAs at 2, 77, 140, 210, and 300 K using data obtained by Density Functional Theory (DFT) calculations at the corresponding temperatures.

INTRODUCTION

GaAs-based photocathodes activated to NEA is the sole existing technology that can deliver intense and highly spin-polarized electron beams for the forthcoming Electron-Ion Collider as well as enable Spin-Polarized Scanning Tunneling Microscopy (SP-STM), Spin-Polarized Low-Energy Electron Microscopy (SP-LEEM) and Diffraction (SP-LEED), and other cutting-edge experiments. These applications have many requirements for photocathodes, including a high ESP and QE.

It has been experimentally observed that the degree of ESP can be increased and even exceed the theoretical maximum of 50 % in a *p*-doped unstrained GaAs cooled to low temperatures [1]. Strained GaAs samples can achieve ESP levels as high as 92 % [2], although this major increase in ESP typically comes at the cost of QE. Maximizing the desirable beam properties like QE, ESP, and photocathode lifetime in parallel has not been achieved [3]. Therefore, the availability of effective modeling tools which can be used to strengthen our understanding of the processes which affect the performance of conventional spin-polarized electron sources is of the utmost importance. This work aims to expand the previously developed spin-polarized Monte Carlo model [4] by incorporating low-temperature and strained-lattice effects in GaAs and provide a foundation for modeling photoemission from novel spin-polarized materials and complex layered structures.

CALCULATION DETAILS

Monte Carlo Modeling

The spin-polarized Monte Carlo model [4] is based on the implementation of three fundamental steps of photoemission: photoexitation of electrons from the valence band (VB) to the conduction band (CB), transport of electrons to the surface of the material, and emission into the vacuum. Photoexcited electrons undergo different scattering mechanisms while moving to the surface, which may change the energy and momentum of the particle and cause a spin flip. The probability of a particular scattering mechanism is determined by its scattering rate, while the probability of a spin flip during that scattering event is defined by the spin-relaxation rate. Further description and implementation details can be found in [4].

The Monte Carlo model accounts for the subtleties of the material band structure and thus requires knowledge of band-structure parameters dependent on crystal temperature, doping density, and lattice strain. These parameters can be obtained from the DFT calculations.

DFT Calculations

DFT calculations can successfully predict various macroscopic properties of materials, only needing the crystal structure as input. In the case of mott insulators, for which the correlation of spin attributes of the material makes their electrical properties deviate from classical predictions, DFT calculations tend to over-delocalize valence electrons and over-stabilize conduction bands, resulting in smaller intrinsic energy gaps than what is observed experimentally. To combat this shortcoming, the Hubbard correction takes into account the energy contributions of spin correlations which enables for more accurate calculations for such materials. The Hubbard correction approach has been implemented in this study using QUANTUM ESPRESSO [5] program

* z2011343@students.niu.edu
† chubenko@niu.edu

ISBN: 978-3-95450-247-9 ISSN: 2673-5490 doi: 10.18429/JACoW-IPAC2024-WEPC65

package to obtain accurate predictions of the GaAs band structure and dielectric permittivity. The phonon dispersion calculation was carried out using non-local norm-conserving pseudopotential from the QUANTUM ESPRESSO pseudopotential library. The complex dielectric permittivity was calculated using the same norm-conserving method as the phonon calculations.

RESULTS AND DISCUSSION

The results of the DFT calculations are compared to available experimental measurements and are contained in Table 1. To benchmark our model, we first model electron transport at different temperatures and compare our results to experimental measurements. Electron drift velocity as a function of electric field strength at multiple temperatures is shown in Fig. 1 along with experimental results obtained from [6]. The simulation was done using the DFT parameters from Table 1, with the exception of Γ effective mass, intrinsic energy gap, band splittings, and dielectric constants, as these parameters were determined to be critical to achieving better agreement with experimental measurements. Experimental values from Table 1 were used for these parameters. Additionally, an electron affinity (EA) of 0.67 eV was employed in all cases. We can see that in addition to displaying the correct temperature dependence, the simulated drift velocities are well within an order of magnitude with respect to the experimental results.

QE as a function of photon energy is shown in Figs. 2 and 3 at temperatures 300 K and 77 K respectively, with the simulation results plotted with the results obtained by Liu *et al.* [1] at three different doping densities. We can see that our results are within an order of magnitude to experimental results and display the correct temperature dependence w.r.t doping density. Figures 4 and 5 show the ESP as a function of photon energy for the same temperatures and doping levels as the QE results.

CONCLUSION

Using the Monte Carlo approach and details of the material band structure determined through DFT simulations in

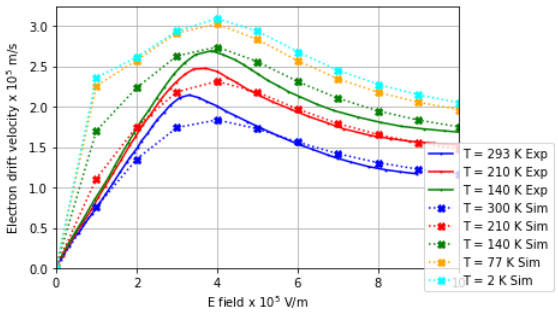

Figure 1: Simulated drift velocity of electrons with varying temperature using band structure parameters obtained from both DFT calculations and experiment, compared to results from [6].

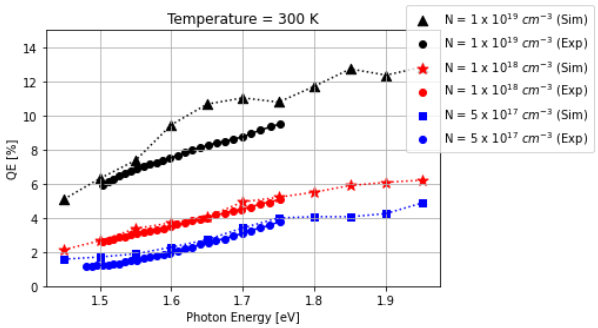

Figure 2: Simulated QE vs. photon energy at room temperature compared to experimental results from [1].

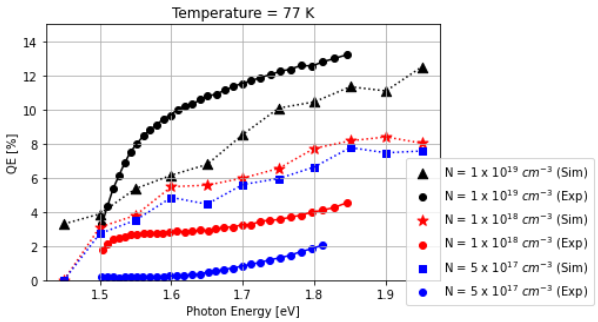

Figure 3: Simulated QE vs. photon energy at T = 77K compared to experimental results from [1].

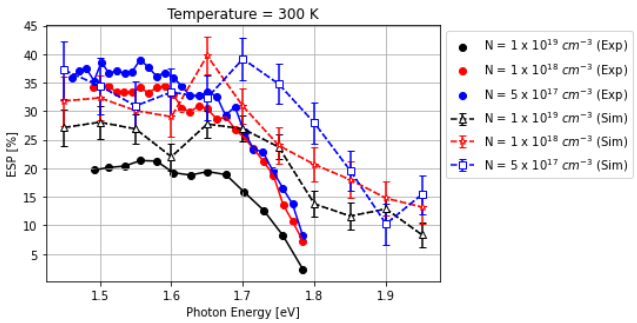

Figure 4: Simulated ESP vs. photon energy at T = 300K compared to experimental results from [1].

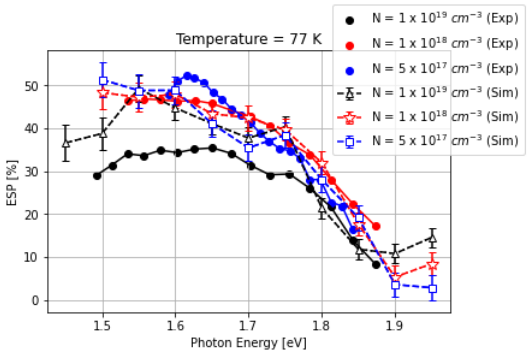

Figure 5: Simulated ESP vs. photon energy at T = 77K compared to experimental results from [1].

ISBN: 978-3-95450-247-9 ISSN: 2673-5490 doi: 10.18429/JACoW-IPAC2024-WEPC65

Table 1: Band structure parameters at multiple temperatures obtained through DFT calculations along with experimental results available in literature

Parameter	**2 K**	**2 K**	**77 K**	**77 K**	**140 K**	**140 K**	**210 K**	**210 K**	**293 K**	**293 K**
	DFT	**Ref.**	**DFT**	**Ref.**	**DFT**	**Ref.**	**DFT**	**Ref.**	**DFT**	**Ref.**
Electron's eff. mass (m_0)										
m_X	0.239		0.239		0.239		0.240		0.240	0.58 [4]
m_Γ	0.079	0.0674 [7]	0.079	0.0672 [7]	0.079	0.0667 [7]	0.079	0.0661 [7]	0.076	0.063 [4]
m_L	0.222		0.222		0.222		0.222		0.222	0.22 [4]
m_{HH}	0.322		0.323		0.323		0.324		0.324	0.51 [4]
m_{LH}	0.099		0.099		0.098		0.098		0.097	0.088 [4]
m_{SO}	0.175		0.175		0.174		0.174		0.173	0.063 [4]
E gap (eV)										
E_g	1.521	1.519 [8]	1.520	1.507 [9]	1.513	1.488 [9]	1.500	1.461 [9]	1.485	1.42 [4]
E_{SO}	0.3722		0.3721		0.3721		0.3720		0.3719	0.34 [4]
Splitting energy (eV)										
Γ - L	0.162	0.296 [10]	0.163	0.295 [10]	0.167	0.292 [10]	0.174	0.289 [10]	0.183	0.29 [4]
Γ - X	0.612	0.462 [10]	0.613	0.464 [10]	0.621	0.467 [10]	0.634	0.471 [10]	0.649	0.48 [4]
Nonparab. factor (eV^{-1})										
α_Γ	0.558		0.559		0.562		0.567		0.573	0.61 [4]
α_L	0.360		0.360		0.361		0.362		0.363	0.461 [4]
α_X	0.272		0.272		0.272		0.271		0.271	0.204 [4]
Dielectric constants (ϵ_0)										
ϵ_∞	10.002	10.58 [11]	10.004	10.67 [11]	10.015	10.75 [11]	10.034	10.84 [11]	10.058	10.92 [4]
ϵ_0	12.208	12.46 [11]	12.211	12.54 [11]	12.227	12.62 [11]	12.255	12.74 [11]	12.290	12.9 [4]
Interv. scat. ph. E (meV)										
Γ → L	29.36		29.35		29.32		29.27		29.21	27.8 [4]
Γ → X	29.89		29.88		29.84		29.76		29.66	29.9 [4]
L→ L	29.36		29.35		29.32		29.27		29.21	29.0 [4]
L → X	21.38		21.37		21.31		21.21		21.08	29.3 [4]
X → X	29.89		29.88		29.84		29.76		29.66	29.9 [4]
Other										
$\hbar\omega_0$ (eV)	33.71		33.70		33.66		33.60		33.52	35.36 [4]
ρ (kg m^{-3})	5344		5343		5338		5329		5319	5360 [4]
ν (m s^{-1})	5213		5224		5227		5231		5236	5240 [4]

QUANTUM ESPRESSO, the photoemission model has been implemented to calculate electron drift velocity, QE, and ESP at multiple temperatures. The preliminary simulation results are within an order of magnitude of expected values and display remarkable accuracy with respect to the temperature dependence of the experimental results. Nonetheless, discrepancies between our DFT parameters and experimental results suggest that further adjustments are required to achieve more accurate results for QE and ESP. Additionally, a detailed understanding of the temperature dependence of electron affinity in *p*-doped GaAs will provide further insight for improving the accuracy of the model.

ACKNOWLEDGEMENTS

This work was performed under the Chicagoland Accelerator Science Traineeship (CAST) program sponsored by the U.S. DOE award DE- SC0020379 to the Illinois Institute of Technology (IIT) and Northern Illinois University (NIU). O. C. and S. K. were supported by the U.S. National Science Foundation under Award PHY-1549132, the Center for Bright Beams. J. O. M.-N. and L. C. were supported by Brookhaven Science Associates, LLC under Contract DE-SC0012704 with the U.S. DOE. J. O. M.-N. thanks Ratnakar Palai for the support in learning QUANTUM ESPRESSO.

ISBN: 978-3-95450-247-9 ISSN: 2673-5490 doi: 10.18429/JACoW-IPAC2024-WEPC65

REFERENCES

[1] W. Liu, M. Poelker, X. Peng, S. Zhang, and M. Stutzman, "A comprehensive evaluation of factors that influence the spin polarization of electrons emitted from bulk GaAs photocathodes," *J. Appl. Phys.*, vol. 122, p. 035 703, 2017. doi:10.1063/1.4994306

[2] X. Jin, B. Ozdol, M. Yamamoto, A. Mano, N. Yamamoto, and Y. Takeda, "Effect of crystal quality on performance of spin-polarized photocathode," *Appl. Phys. Lett.*, vol. 105, no. 20, 2014. doi:10.1063/1.4902337

[3] J. K. Bae, A. Galdi, L. Cultrera, F. Ikponmwen, J. Maxson, and I. Bazarov, "Improved lifetime of a high spin polarization superlattice photocathode," *J. Appl. Phys.*, vol. 127, no. 12, p. 124 901, 2020. doi:10.1063/1.5139674

[4] O. Chubenko *et al.*, "Monte carlo modeling of spin-polarized photoemission from p-doped bulk GaAs," *J. Appl. Phys.*, vol. 130, no. 6, p. 063 101, 2021. doi:10.1063/5.0060151

[5] P. Giannozzi *et al.*, "QUANTUM ESPRESSO: A modular and open-source software project for quantum simulations of materials," English (US), *Journal of Physics Condensed Matter*, vol. 21, no. 39, 2009. doi:10.1088/0953-8984/21/39/395502

[6] J. G. Ruch and G. S. Kino, "Transport properties of GaAs," *Phys. Rev.*, vol. 174, no. 3, pp. 921–931, 1968. doi:10.1103/PhysRev.174.921

[7] H. Hazama, T. Sugimasa, T. Imachi, and C. Hamaguchi, "Temperature dependence of the effective masses in III-V semiconductors," *J. Phys. Soc. Jpn.*, vol. 55, no. 4, p. 1282, 1986. doi:10.1143/JPSJ.55.1282

[8] J. Blakemore, "Semiconducting and other major properties of gallium arsenide," *J. Appl. Phys.*, vol. 53, pp. 123–181, 1982. doi:10.1063/1.331665

[9] C. D. Thurmond, "The standard thermodynamic functions for the formation of electron and hole in Ge, Si, GaAs and GaP," *J. Electrochem. Soc.*, vol. 122, pp. 133–141, 1975. doi:10.1149/1.2134410

[10] D. E. Aspnes, "GaAs lower conduction-band minima: Ordering and properties," *Phys. Rev. B*, vol. 14, no. 12, pp. 5331–5343, 1976. doi:10.1103/14.5331

[11] I. Strzalkowski, S. Joshi, and C. Crowell, "Dielectric constant and its temperature dependence for GaAs, CdTe, and ZnSe," *Appl. Phys. Lett.*, vol. 28, p. 350, 1976. doi:10.1063/1.88755